A Murine Model of Abductor Insufficiency Accelerates the Development of Hip Osteoarthritis

Michael B. Geary MD[1]*, Caitlin A. Orner MD[1]*, Helen Shammas[1,3], John M. Reuter[1,2], Alayna E. Loiselle PhD[1,2], Chia-Lung Wu PhD[1,2#†], Brian D. Giordano MD[1,2#]

*co-first authors
co-last authors
† corresponding Author

[1] Center for Musculoskeletal Research
University of Rochester Medical Center
601 Elmwood Avenue, Box 665, Rochester, NY 14642, USA

[2]Department of Orthopaedics and Rehabilitation
University of Rochester Medical Center
601 Elmwood Avenue, Box 665, Rochester, NY 14642, USA

[3]Department of Biomedical Engineering
University of Rochester Medical Center
601 Elmwood Avenue, Box 665, Rochester, NY 14642, USA

Corresponding Author:
Chia-Lung Wu PhD

Abstract

Osteoarthritis (OA) of the hip is a common and debilitating painful joint disease. A growing body of evidence suggests that there may be an association between periarticular myotendinous pathology and the development of hip OA. Thus, we hypothesized that a murine model of hip OA could be achieved through selective injury of the abductor complex around the hip. C57BL6/J mice were randomized to sham surgery or abductor injury, in which the myotendinous insertion at the third trochanter and greater trochanter were surgically detached. Mice were allowed free, active movement until sacrifice at either 3 weeks or 20 weeks post-injury. Histologic analyses and immunohistochemical staining (IHC) of the femoral head articular cartilage were performed, along with μCT analysis to assess subchondral bone remodeling. We observed that mice receiving abductor injury exhibited significant OA severity with loss of Type II Collagen staining compared to sham control mice at 20 weeks post-surgery, comparable MMPI13 expression was observed between injury and sham groups. No significant differences in subchondral bone were found on μCT after 20 weeks following injury. Our study suggests a link between abductor dysfunction and the development of hip OA, which are common pathomorphologies encountered in routine orthopaedic clinical practice. Further, this novel animal model may provide a valuable tool for future investigations into the pathogenesis and treatment of hip OA.

Keywords: Osteoarthritis, hip, abductor, gluteus medius, proteoglycan

Introduction

Osteoarthritis (OA) affects over 32.5 million people in the United States, and approximately 10% of adults over the age of 45 will suffer from symptomatic hip OA at some point in their life[1]. The hip is the second most commonly affected large joint, after the knee[2]. Hip OA is generally divided into primary idiopathic causes, and secondary causes resulting from an identifiable factor[3]. Secondary degeneration of the hip can result from a number of pathologies, including inflammatory diseases such as rheumatoid arthritis, and has been linked to structural pathomorphologies such as femoral acetabular impingement (FAI)[4]. Despite much study on the causative factors related to the onset and progression of hip OA, the underlying etiology remains to be elucidated.

The hip is a diarthrodial joint that allows for multidirectional range of motion. The periarticular musculature of the hip, in particular the gluteus medius and minimus and their associated tendons, contribute to dynamic stability of the joint. It is well-recognized that altered arthrokinematics negatively influence articular cartilage loading and contributes to the progression of OA. Multiple studies have observed an association between periarticular tendinopathy and hip OA, without definitively establishing causality[5,6]. In a clinical study, a small series of patients with abductor tears were found to demonstrate a high rate of concomitant intra-articular injury[7]. Therefore, these studies provided rationale for considering whether musculotendinous dysfunction or injury surrounding the hip may lead to the development of OA.

Animal models of pathogenesis of hip joint and OA mostly utilize large animals including cannies[8-10], sheep[11], and porcine[12] with the advantage of large animals having similar cartilage morphology, thickness as well as the responses to injury to humans[13-15]. These large animal hip

47 OA models not only have already provided us invaluable insights into hip cartilage physiology
48 and pathophysiology but also serve as essential pre-clinical models for drug development.
49 Despite these benefits, large animals are not amenable to the power of genetic modification to
50 better define the cellular and molecular etiology of pathogenesis, as can be conducted in mice[15].
51 Furthermore, there is a paucity of literature on murine hip injury models[16]. The purpose of the
52 present study, therefore, was to establish a novel murine model of hip OA induced by abductor
53 injury and determine whether an association exists between abductor insufficiency and hip OA
54 onset and progression. We hypothesize that abductor injury accelerates the development of hip
55 OA. OA severity, subchondral bone remodeling, as well as anabolic and catabolic biomarkers
56 were evaluated by histology, immunohistochemistry (IHC) and uCT analyses in the current
57 study.
58

59 **Materials and Methods**

60 ***Animal Model of Abductor Instability***

61 All animal procedures were approved by the University Committee on Animal Research
62 (UCAR) at the University of Rochester. Female C57BL/6J mice (8-10 weeks-old; #00664,
63 Jackson Laboratories, Bar Harbor, ME) weighing on average between 20 and 25 g were
64 anesthetized by intraperitoneal injection of ketamine (60 mg/kg) and xylazine (4 mg/kg). The
65 hind region and right leg were shaved and prepared with alcohol and betadine (povidone-iodine).
66 The proximal femur was approached through a 1 cm lateral skin incision placed over the third
67 trochanter, followed by a direct incision through the fascial layer, exposing the underlying third
68 and greater trochanters.
69

70 Mice were randomly divided into two groups. One group received abductor injury, while the
71 other group received sham surgery. The effect of abductor injury on hip OA development was
72 investigated at two time points following surgery: 3 weeks and 20 weeks post-surgery. n = 4-5
73 mice per group (sham or surgery) per time point. The sham group underwent anesthesia along
74 with incisions of the skin and fascia. A Schematic diagram of the right proximal femur shows the
75 locations of the femoral head (FH), greater trochanter (GT), lesser trochanter (LT), third
76 trochanter (3T), and sciatic nerve (SN) (**Fig. 1A**). Coronal μCT reconstruction of the right hip
77 demonstrates the anatomic positions of the FH and GT (**Fig. 1B**). The injury group had release
78 of the muscular attachments to the 3T (**Fig. 1C**) as well as detachment of the large abductor
79 complex (ABD) from the GT (**Fig. 1D**). During each surgery, careful attention was paid to avoid
80 injury to the SN running posterior to the proximal femur. For all mice, the fascial layer was
81 closed with a single 5-0 nylon suture (Ethicon, Inc.), and the skin was closed with either 7 mm
82 stainless steel wound clips (CellPoint Scientific Inc., Gaithersburg, MD) or a series of interrupted
83 5-0 nylon sutures. For analgesia, mice were given subcutaneous buprenorphine (0.05 mg/kg) at
84 the time of surgery and each subsequent day over the following 72 hours. Following surgery,
85 mice were returned to their cage and allowed free active motion and weight bearing. Animals
86 were monitored daily until sacrifice.
87
88 ***Evaluation of bone tomography***
89 Mice were sacrificed at either 3-weeks or 20-weeks post-surgery (n = 4 -5 per group per time
90 point). Immediately after sacrifice, the hemi-pelvis and femur were prepared by removing the
91 skin and excess soft tissue, leaving the hip and the major muscular attachments around the pelvis
92 and femur. The samples were fixed for 72 hours in 10% neutral buffered formalin (NBF), then
93 washed, placed in 70% EtOH, and subjected to the μCT scanning. Hips were scanned using the

94 VivaCT 40 system (Scanco Medical, Basserdorf, Switzerland) at highest resolution with a pixel
95 size of 10.5 μm to image bone. An integration time of 300 ms and an X-ray voltage of 55 kVP
96 was used. The hip was captured and segmented using a scanning threshold of 320 to identify
97 bone. The femoral head was analyzed for trabecular bone (excluding cortical) at a threshold of
98 310. Views of the femoral head and acetabulum were analyzed using a threshold of 320. The
99 Gaussian method was used for noise reduction (sigma 0.8 with support value of 1 pixel).
100
101 ***Evaluation of OA severity***
102 Following 72 hours fixation and μCT scanning, samples were decalcified in 14% (pH 7.2)
103 EDTA at room temperature for 2 weeks. Samples were then dehydrated and embedded in
104 paraffin with the posterior surface of the hip facing down. Using the SN as a landmark, serial
105 sections (thickness = 5 μm) were taken through the preserved hip and surrounding soft tissue in a
106 coronal plane. Three different levels were cut through the joint, with five sections taken at each
107 level.
108
109 Safranin O / Fast Green staining was used to visualize changes in the hip articular structure and
110 proteoglycan content of the mice at 3 weeks and 20 weeks post-surgery. Slides were baked
111 overnight at 60°C, then deparaffinized and rehydrated through graded ethanol. After air drying,
112 slides were stained in Weigert's Hematoxylin for 7 minutes (Equal parts Solution A, CAS# 517-
113 23-2 and Solution B, CAS# 7705-08-0) then rinsed with running tap water. Slides were stained
114 with 0.02% Fast Green (CAS# 2353-45-9) for 3 minutes, rinsed in 1% acetic acid for 10 seconds,
115 then stained with 1% Safranin O (CAS# 477-23-6) for 5 minutes. After a quick rinse in 0.5%
116 acetic acid and rinses with double-distilled water, slides were then air dried and cover slipped.
117

118 OA severity was determined by modified Mankin scoring system as previously described[17].
119 Three independent, blinded graders assessed sections for degenerative changes in the hip
120 articular cartilage. Scores including articular structure (0-11), tidemark (0-3), loss of
121 proteoglycan staining (0-8), and chondrocyte clones (0-2) were averaged among graders for the
122 hip femoral head, resulting in total scores between 0 and 24.
123
124 ***Immunohistochemistry***
125 Immunohistochemistry (IHC) was performed for Collagen Type II A1 (COL2A1) and Matrix
126 Metalloproteinase 13 (MMP13). For both protocols, slides were baked overnight at 60°C, then
127 deparaffinized and rehydrated through graded alcohols. IHC labeling for MMP13 (Thermo
128 Fischer Scientific, Waltham, MA. Catalog #MS-825P) began with enzymatic antigen retrieval
129 using hyaluronidase (Sigma-Aldrich, St. Louis, MO; H-3506) for 10 minutes in a 37°C water
130 bath. Endogenous peroxidase was then quenched for 30 minutes using endogenous blocking
131 reagent (Dako North America, Carpinteria, CA; S2003). After rinses with deionized water and
132 PBS-T, slides were blocked for 30 minutes with 5% Normal Horse Serum (NHS; Vectastain
133 Elite ABC Kit (Mouse IgG), Vector Laboratories, Burlingame, CA; PK-6102), then with the
134 Blocking Endogenous Antibody Technology (BEAT) kit (Invitrogen Corporation, Camarillo,
135 CA; 50-300). Overnight incubation with the primary antibody (Thermo Fischer Scientific,
136 Waltham, MA; MS-825P; 1:200) was done at 4°C, with control slides incubated with mouse IgG
137 at the same concentration (1ug/mL). On the second day, sections were incubated with the
138 secondary antibody (Vector PK-6102), then ABC reagent (Vector PK-6102). Color was detected
139 using Vector DAB ImmPACT kit (Vector SK-4105), then counterstained with hematoxylin.
140

141 IHC labeling for COL2A1 was performed as follows. Enzymatic antigen retrieval was performed
142 for 10 minutes in a 37°C water bath using pepsin (Sigma-Aldrich, P7000). After rinses, sections
143 were blocked with endogenous blocking reagent (Dako, S2003) for 30 minutes, then with 5%
144 NHS (Vector PK-6102) for 30 minutes. The primary antibody (Thermo Scientific, MS235-P;
145 1:100) was left to incubate at 4°C overnight, with control slides incubated with the same
146 concentration of mouse IgG (2ug/mL). On the second day, sections were incubated with the
147 secondary antibody (Vector PK-6102) and ABC reagent (Vector PK-6102), then color was
148 detected with the Vector DAB ImmPACT kit (Vector SK-4105) counterstained with
149 hematoxylin.
150
151 ***Statistics***
152 To determine how surgery, time (following surgery), and their interaction (surgery x time)
153 affected hip OA severity, as well as subchondral bone remodeling, data were analyzed by two-
154 way repeated measures ANOVA following by Sidak's multiple comparisons test ($\alpha = 0.05$) using
155 GraphPad Prism version 9. Values are expressed as mean ± SD.
156
157 ***Source of Funding***
158 This study was supported by NIH AR075899 (CLW), OREF Etiology of Hip Osteoarthritis
159 Grant (CLW & BG) as well as Goldstein Award (BG) through the University of Rochester's
160 Department of Orthopaedics and Rehabilitation. MBG was supported by CTSA (TL1 TR000096)
161 from NIH/NCATS. CAO was supported by the University of Rochester Office for Medical
162 Education Year-Out Research Fellowship. The HBMI and BBMTI cores are supported by
163 NIH/NIAMS P30 AR069655.
164

165 **Results**

166 ***Mice receiving abductor surgery demonstrated significantly increased OA severity compared***
167 ***to sham group 20 weeks following injury.***

168 Safranin-O is a cationic dye that stains proteoglycans, and intensity of red Safranin-O staining is
169 a proxy for proteoglycan content. Loss of proteoglycan content is a clinical hallmark of OA[18].
170 Hips from the sham and injured groups were stained at 3 weeks and 20 weeks post-injury with
171 Safranin-O/Fast Green to visualize proteoglycans. After 20 weeks, mice in the injured group
172 demonstrated loss of proteoglycan staining of the articular surface relative to sham, although
173 articular cartilage surface was comparable between two groups (**Fig. 2A-B**). No significant
174 differences in OA severity was observed between sham and injured groups at 3 weeks post-
175 injury. Furthermore, sham mice had similar OA severity at 3 weeks and 20 weeks post-surgery.
176

177 ***Mice receiving abductor surgery exhibited decreased COL2A1 staining but comparable***
178 ***MMP13 staining in the articular cartilage relative to sham mice at 20 weeks following***
179 ***abductor injury***

180 IHC labeling for COL2A1 and MMP13 in articular cartilage of the femoral head was performed
181 at 20 weeks post-injury as this was the timepoint when OA was evident in the mice receiving
182 surgery. In the sham group, a superficial layer of unmineralized cartilage is characterized by
183 pericellular staining of COL2A1 (**Fig. 3A-B**). In the deeper layers, staining intensity is increased
184 and more evenly distributed throughout the extracellular matrix. Hips from the injury group
185 show a notable decrease in staining intensity in the uncalcified articular cartilage, relative to
186 sham mice.

187 MMP13 has been shown to play a catabolic role in OA[19], and increased staining of MMP13 has
188 been observed in animal models of arthritis[20,21]. IHC staining for MMP13 was performed to

189 visualize changes in femoral head articular cartilage after sham surgery and abductor injury.
190 There was no appreciable staining for MMP13 in the articular cartilage at 20 weeks post-injury
191 in the both sham and surgery groups (**Fig. 3**).
192
193 ***µCT reveals no significant change in subchondral bone parameters 20 weeks post-injury***
194 To evaluate potential structural changes in subchondral bone, hips from the sham group and the
195 injury group were analyzed by µCT to compare subchondral microtrabecular volumetric
196 parameters 3- and 20-weeks following injury (**Fig. 4**). No changes in cancellous bone fraction
197 (bone volume/total volume, BV/TV, excluding the cortex) were detected in the injured group
198 relative to sham at 20 weeks (Sham: 0.51 ± 0.1; Injury: 0.51 ± 0.1) (**Fig. 4A**). In addition, there
199 were no significant differences in trabecular bone characteristics between two groups. This
200 includes trabecular number (Sham: 6.3/mm ± 0.8; Injury: 6.3/mm ± 0.4) (**Fig. 4B**), trabecular
201 thickness (Sham: 79.2 µm ± 8.1; Injury: 81.8 µm ± 7.3) (**Fig. 4C**), and trabecular spacing (Sham:
202 151.8 µm ± 23.5; Injury: 147.5 µm ± 10.8) (**Fig. 4D**).
203
204 **Discussion**
205 With the growth in clinical evidence indicating an association between abductor insufficiency
206 and the development of hip OA, it is essential to develop a reproducible small animal model that
207 allows scientists to study the pathogenesis of this linked disease process[5,6]. To date, however,
208 only a few rodent hip OA models have been established and can be generally categorized into
209 either chemically-induced or surgically-induced OA[16,22]. Intra-articular injection of monosodium
210 Iodoacetate (a chondrocyte glycolytic inhibitor) exhibited rapid hip OA development compared
211 to controls within 14 days in a rat model. However, it is not clear whether such a progressive and
212 destructive OA phenotype is representative of chronic hip OA in humans[22]. In another study,

213 various degrees of hip instability ranging from mild, moderate, severe to femoral head resection
214 were surgically induced in mice at weaning (3-week-old neonatal pups)[16]. Their data suggest that
215 hip instability induced by loss-of-function of soft connective tissue led to morphometric changes
216 in the growing mouse hip. However, understanding how abductor injury may induce OA in the
217 context of a skeletally mature hip (as indicated fusion of triradiate cartilage of the pelvis)[23], has
218 remained a key knowledge gap to this point. Furthermore, our small animal hip OA model may
219 be used to explore the sequence of pathoanatomical and anabolic/carbolic effects on OA onset
220 and progression.
221
222 Animal models of surgical OA require well-established techniques that can be easily
223 reproduced[13]. In this model the third trochanter (3T) serves as a surgical landmark, which can be
224 palpated before making the skin incision. Once the muscular attachments to the 3T have been
225 cut, the femur is followed proximally to the large abductor complex on the greater trochanter
226 (GT). These muscles are easily visualized, and can be cleanly cut without injuring surrounding
227 structures. The surgery avoids dissecting around deep structures; the major potential injury is to
228 the sciatic nerve (SN) running posterior to the proximal femur. In preliminary work, we
229 experimented with performing a capsulotomy to induce an even greater severity of injury.
230 Through multiple surgeries, we found that the capsule in the mouse may be too small to reliably
231 incise without risking damage to the sciatic nerve running in close approximation to the joint. As
232 such, this group has been excluded from the presented results.
233
234 The primary findings in this study were the loss of proteoglycan and COL2A1 staining in
235 uncalcified articular cartilage 20 weeks after injury. Loss of proteoglycan and type II collagen

236 contents are both histologic hallmarks of OA, and the observations made in the injured group
237 after 20 weeks suggest that OA progression is accelerated after abductor injury. Additionally,
238 sham mice had similar OA severity at 3 weeks and 20 weeks post-surgery, suggesting that both
239 sham surgery and aging (i.e. ~ 6 moths of age) were not sufficient to induce hip OA onset.
240 Interestingly, no changes in MMP13 IHC staining were observed between the sham and injured
241 groups, suggesting that either MMP13 may not be the main catabolic mediator in our mouse hip
242 OA model or other timepoints may need to be investigated in order to establish temporal
243 expression pattern of MMP13. Indeed, our results are also consistent with the findings from the
244 study of Killian *et al*. where the authors indicated low MMP13 staining in articular cartilage in
245 their titrated model of hip dysplasia. Future studies investigating other cartilage degradation
246 enzymes, such as ADAMTS4, MMP3, MMP9, etc., as well as additional timepoints post-surgery
247 are warranted. Radiographic analysis of subchondral bone remodeling did not reveal significant
248 differences between sham and injured groups at any time point investigated in this study.
249 Nevertheless, long-term study may be required to observe subchondral bone remodeling in our
250 mouse model.
251
252 The gluteus medius and minimus, in conjunction with the tensor fascia lata and gluteus maximus,
253 represent the main components of the hip abductor complex. This complex contributes to the
254 "contractile layer" of the hip, and is thought to exert considerable influence on the intraarticular
255 joint space and its associated layers[24]. In a clinical outcome study that evaluated the results of
256 arthroscopic gluteus medius/minimus repairs, a high incidence of concomitant intraarticular hip
257 pathology was noted[7]. Abductor tendon pathology leads to considerable pain and functional
258 impairment. Both open and arthroscopic repair techniques have been proposed and excellent

259 clinical results have been reported for both repair types [7,25,26]. The causal relationship between
260 periarticular myotendinous pathology and the onset and progression of OA is intriguing but
261 remains understudied. Emerging clinical data for the hip joint support the association between
262 pathology of the extra-articular soft tissue envelope and intra-articular joint disease. Therefore,
263 reestablishment of an effective abductor force coupling mechanism may help to optimize and re-
264 balance loading characteristics and potentially influence the progression of intraarticular
265 degenerative changes that may ultimately result in the need for joint arthroplasty.
266
267 The true incidence of abductor tears and/or tendinosis in the general and athletic population
268 remains unknown. In addition, the natural history of untreated tears is unclear. Some studies
269 have observed an association between hip abductor disease and OA [5,27]. A recent histologic study
270 evaluated the ultrastructure of the abductor tendon complex in 10 patients treated for displaced
271 femoral neck fractures and 10 patients undergoing total hip arthroplasty for OA. All of the
272 patients treated for OA were found to have coexisting tendinosis, with prominent scarring and
273 overall greater degenerative changes than the group treated for traumatic fractures of the femoral
274 neck[6]. While not clearly establishing that tendon pathology contributes to OA, these observations
275 raise important questions regarding the relationship between these two pathologies. It is likely
276 that abductor compromise, through an analogous pathomechanical process, may contribute to the
277 onset and progression of hip OA.
278
279 While our present study establishes a reproducible injured-induced mouse hip OA model and
280 offers an important step forward in investigating the role of abductor insufficiency in the
281 development of hip OA, there are limitations that must be considered. First, the mechanisms
282 underlying myotendinous pathology and abductor insufficiency leading to mouse hip OA

283 development remain to be determined. Particularly, to what extent the biomechanical loading on
284 the hip cartilage and mouse behaviors such as gaits and weight bearing are altered following
285 abductor surgery need to be quantified in the future. An additional limitation that must be
286 considered is the clinical relevance of a quadruped model for hip OA, as weight bearing is
287 distributed across four limbs in mice, and thus, gait and biomechanics differ from humans.
288 Despite this limitation, mice and humans share similar joint congruence at the hip.
289
290 In conclusion, we have established a novel murine model of surgically-induced hip OA through
291 an injury to the abductor complex around the hip. Furthermore, this model may be utilized as a
292 valuable tool to examine potential biomarkers associated with hip OA progression[28]. We believe
293 that for the broader orthopaedic community of clinicians and researchers, our findings will
294 increase understanding the role of abductors in hip stability and the development of joint
295 pathology.
296
297 **Acknowledgements**
298 We would like to thank the Histology, Biochemistry and Molecular Imaging (HBMI) and
299 Biomechanics, Biomechanics and Multimodal Tissue Imaging (BBMTI) cores in the Center for
300 Musculoskeletal Research (CMSR) for technical assistance. We appreciate the gracious
301 generosity of the Goldstein Family, who supported the Goldstein Award which provided funding
302 for this work. We also thank Dr. Victoria Hansen and Gulzada Kulzhanova's assistance on
303 performing modified Mainkin score grading for hip joint OA severity for the current project.
304
305 **Author contributions**

306 AL, CLW, and BG conceptualized the study. MBG, CAO, and JR performed mouse surgeries
307 and μCT measurements. HS, JR, CLW, and members in CLW's lab performed modified
308 Mainkin score grading for hip joint OA severity. HS performed IHC staining and imaging. All
309 authors wrote, reviewed, and edited the manuscript.

310 **Figure and Figure Legends**

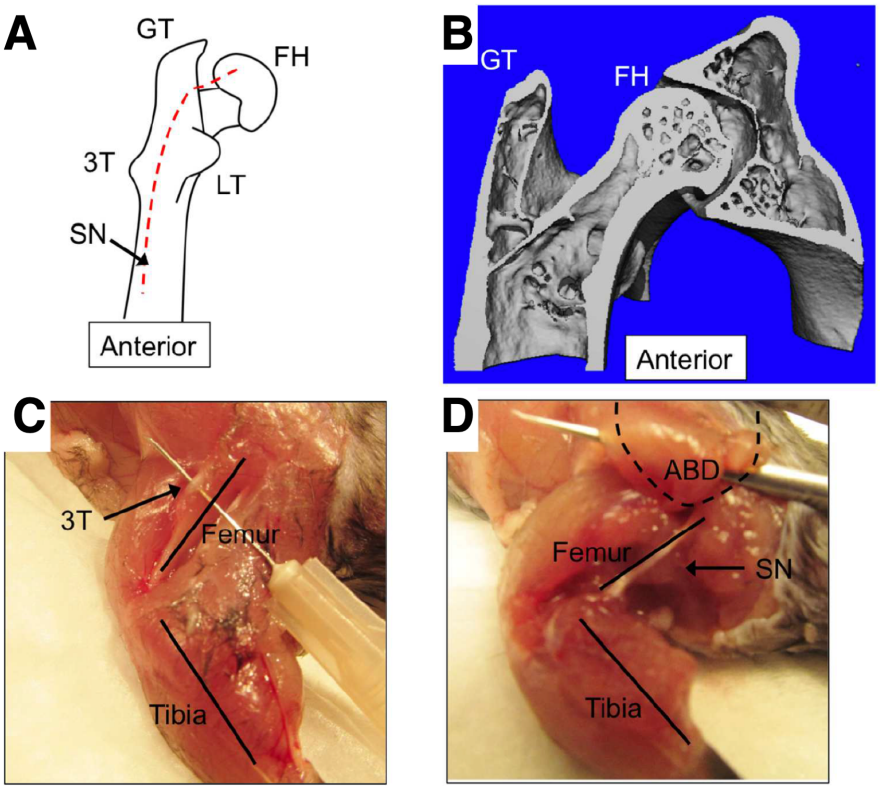

311

312 **Figure 1**. **Surgical model of abductor complex injury**. (**A**) Schematic of the right proximal
313 femur showing the locations of the femoral head (FH), greater trochanter (GT), lesser trochanter
314 (LT), and third trochanter (3T), as well as the path of the sciatic nerve (SN) running posterior to
315 the femur. (**B**) Coronal reconstruction of the right hip showing the anatomic positions of the
316 femoral head (FH) and greater trochanter (GT). (**C**) Photograph of the left hind limb with skin
317 removed. The femur and tibia are labeled for orientation. The third trochanter (3T) is visible
318 superficially, with a needle placed into the muscular attachments. Attachments running proximal
319 from the third trochanter were removed in this injury model. (**D**) Photograph of the left hind limb
320 highlighting the abductor attachments (ABD) to the greater trochanter (dashed outline). The
321 entire abductor complex was detached in the injury group. The femur, tibia, and sciatic nerve
322 (SN) are labeled for orientation.

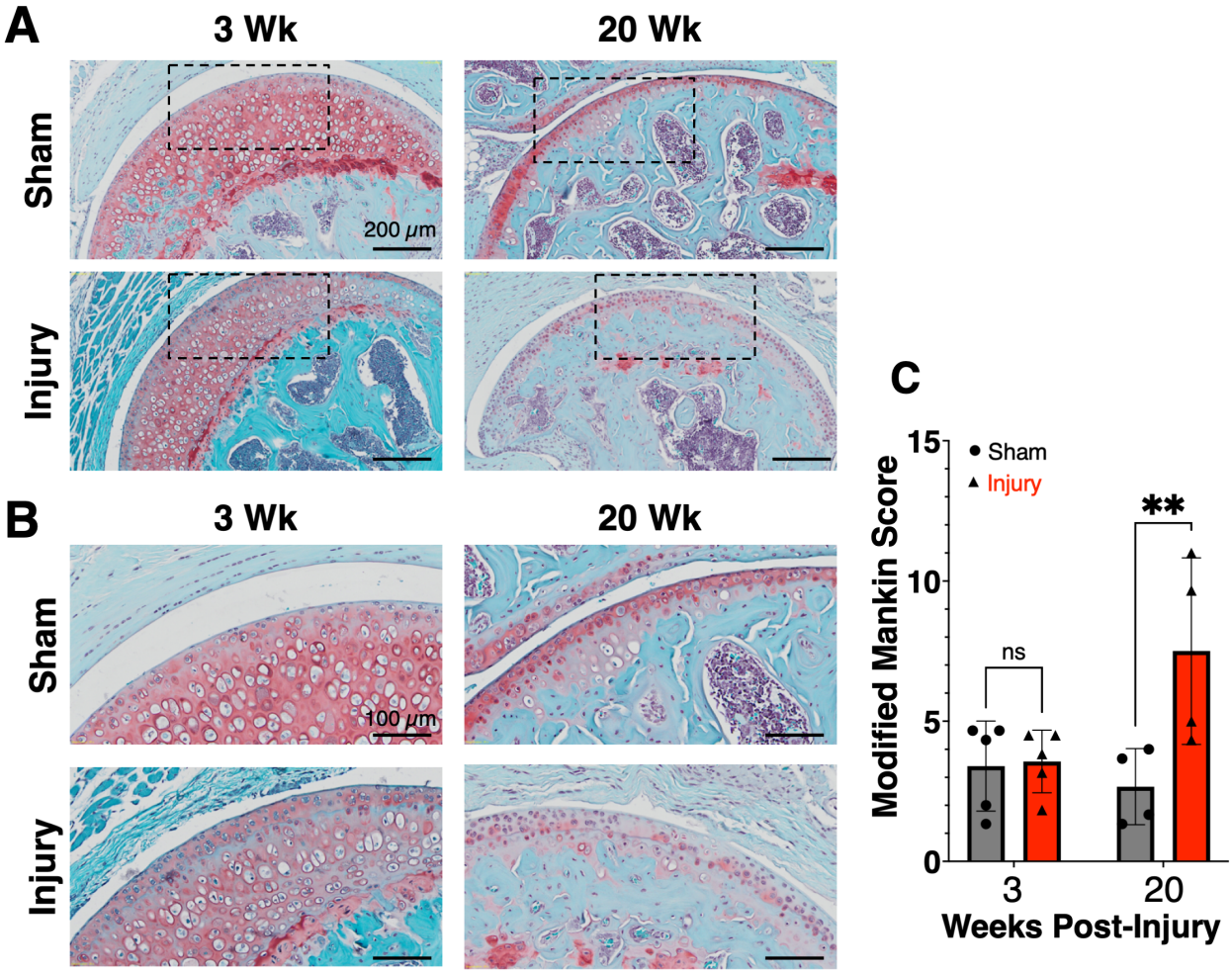

Figure 2. Abductor injury results in loss of proteoglycan staining 20 weeks post-surgery. Coronal sections through the hip were stained with Safranin O/Fast Green, in which proteoglycan stains red. (**A**) Sections are shown for sham and injured groups at 3 and 20 weeks after surgery. Loss of proteoglycan staining is evident in the injured group after 20 weeks relative to sham group. (**B**) Increased magnification of the areas indicated by dashed rectangles in (**A**). (**C**) Modified Mankin scores shows increased OA severity of the mice receiving surgery 20 weeks post-injury as compared to corresponding sham group. Two-way repeated measured ANOVA following by Sidak's multiple comparisons test. Mean ± SD. ns: No statistically significant was detected.

333

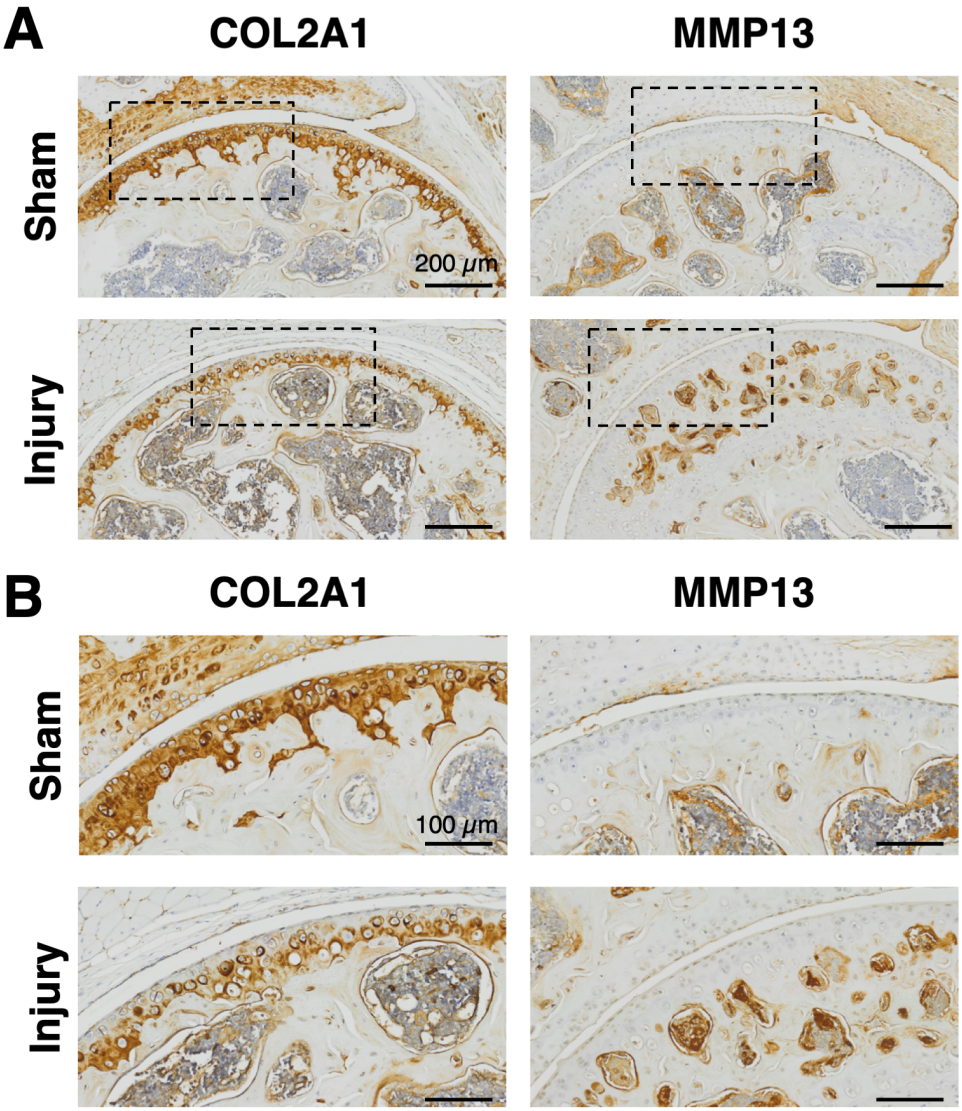

334

335 **Figure 3. COL2A1 and MMP13 staining reveal loss of type II collagen content in the**

336 **unmineralized hip cartilage of the mice 20 weeks post-surgery. (A)** Coronal sections through

337 the hip are shown following IHC for COL2A1 and MMP13 staining. Dark red/brown color

338 indicates positive staining. A substantially decreased COL2A1 staining in the unmineralized hip

339 cartilage of the mice receiving surgery; however, no apparent staining for MMP13 was detected

340 for both sham and surgery groups. (**B**) Increased magnification of the areas indicated by dashed

341 rectangles in (**A**).

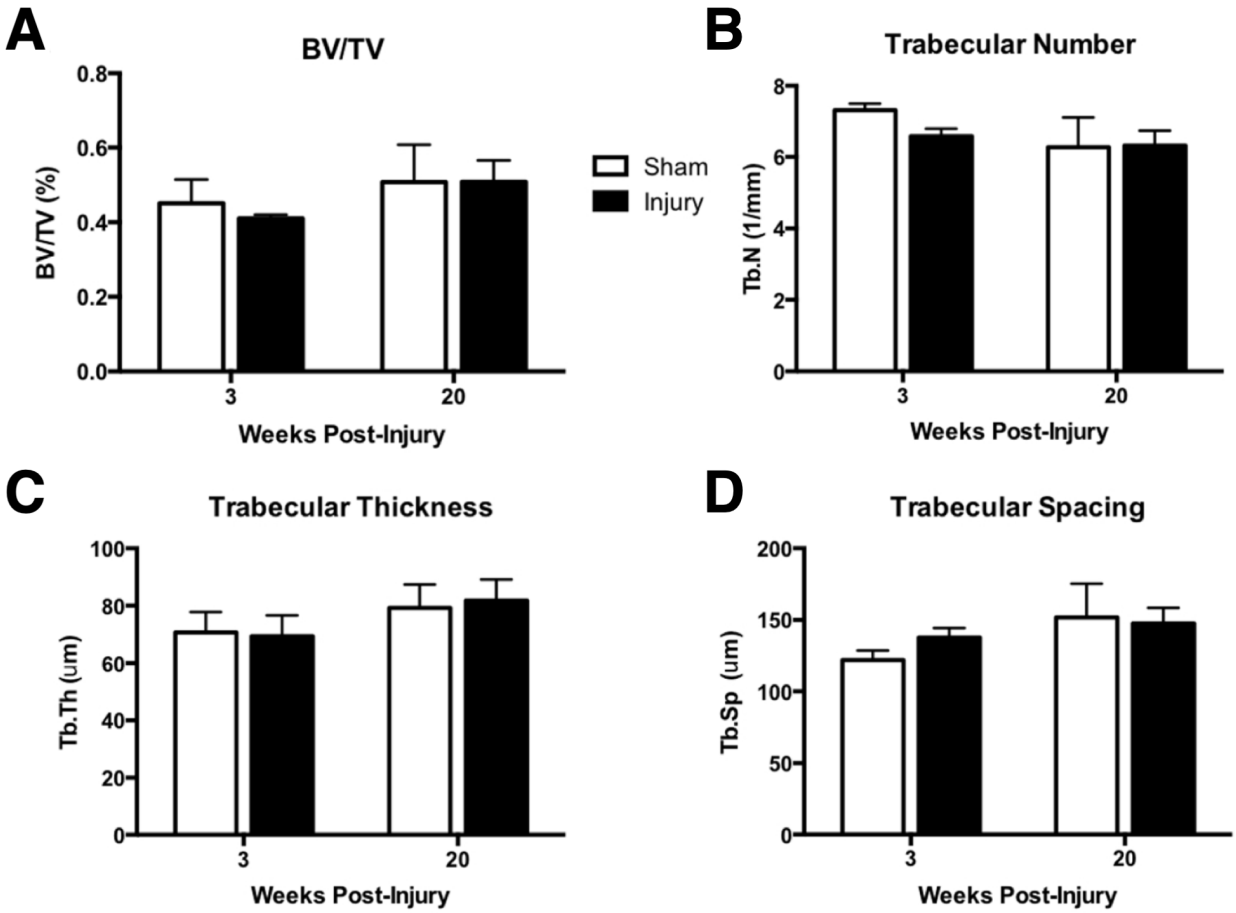

Figure 4. µCT analysis indicates no significant changes in subchondral bone parameters following abductor injury. µCT was used to assess the subchondral bone of the femoral head. (**A**) The ratio of bone volume to total volume (BV/TV), (**B**) Trabecular number, (**C**) trabecular thickness, and (D) trabecular spacing were measured at 3- and 20-weeks post-surgery for bot sham and surgery groups. There are no significant differences in subchondral bone parameters between the two groups in any time point investigated. Two-way repeated measured ANOVA following by Sidak's multiple comparisons test. Mean ± SD.

351 **Reference**

352 1 Lawrence, R. C. *et al.* Estimates of the prevalence of arthritis and other rheumatic
353 conditions in the United States: Part II. *Arthritis & Rheumatism* **58**, 26-35 (2008).
354 2 Zhang, W. *et al.* OARSI recommendations for the management of hip and knee
355 osteoarthritis, part I: critical appraisal of existing treatment guidelines and systematic
356 review of current research evidence. *Osteoarthritis and cartilage* **15**, 981-1000 (2007).
357 3 Hoaglund, F. T. & Steinbach, L. S. Primary osteoarthritis of the hip: etiology and
358 epidemiology. *JAAOS-Journal of the American Academy of Orthopaedic Surgeons* **9**,
359 320-327 (2001).
360 4 Elias-Jones, C. J. *et al.* Inflammation and neovascularization in hip impingement: not just
361 wear and tear. *The American journal of sports medicine* **43**, 1875-1881 (2015).
362 5 Howell, G., Biggs, R. & Bourne, R. Prevalence of abductor mechanism tears of the hips
363 in patients with osteoarthritis. *The Journal of arthroplasty* **16**, 121-123 (2001).
364 6 Meknas, K. *et al.* Could tendinosis be involved in osteoarthritis? *Scandinavian journal of*
365 *medicine & science in sports* **22**, 627-634 (2012).
366 7 Domb, B. G., Botser, I. & Giordano, B. D. Outcomes of endoscopic gluteus medius
367 repair with minimum 2-year follow-up. *The American journal of sports medicine* **41**, 988-
368 997 (2013).
369 8 Pascual‐Garrido, C. *et al.* Canine hip dysplasia: a natural animal model for human
370 developmental dysplasia of the hip. *Journal of Orthopaedic Research®* **36**, 1807-1817
371 (2018).
372 9 Little, D. *et al.* Functional outcome measures in a surgical model of hip osteoarthritis in
373 dogs. *Journal of experimental orthopaedics* **3**, 1-16 (2016).

374 10 Jónasson, P. S. *et al.* Strength of the porcine proximal femoral epiphyseal plate: the effect
375 of different loading directions and the role of the perichondrial fibrocartilaginous
376 complex and epiphyseal tubercle–an experimental biomechanical study. *Journal of*
377 *experimental orthopaedics* **1**, 1-9 (2014).
378 11 Siebenrock, K. A., Fiechter, R., Tannast, M., Mamisch, T. C. & von Rechenberg, B.
379 Experimentally induced cam impingement in the sheep hip. *Journal of orthopaedic*
380 *research* **31**, 580-587 (2013).
381 12 Pawaskar, S. S., Grosland, N. M., Ingham, E., Fisher, J. & Jin, Z. Hemiarthroplasty of hip
382 joint: An experimental validation using porcine acetabulum. *Journal of biomechanics* **44**,
383 1536-1542 (2011).
384 13 Teeple, E., Jay, G. D., Elsaid, K. A. & Fleming, B. C. Animal models of osteoarthritis:
385 challenges of model selection and analysis. *The AAPS journal* **15**, 438-446 (2013).
386 14 Gregory, M. H. *et al.* A review of translational animal models for knee osteoarthritis.
387 *Arthritis* **2012** (2012).
388 15 Oláh, T., Michaelis, J. C., Cai, X., Cucchiarini, M. & Madry, H. Comparative anatomy
389 and morphology of the knee in translational models for articular cartilage disorders. Part
390 II: Small animals. *Annals of Anatomy-Anatomischer Anzeiger* **234**, 151630 (2021).
391 16 Killian, M. L. *et al.* Novel model for the induction of postnatal murine hip deformity.
392 *Journal of Orthopaedic Research®* **37**, 151-160 (2019).
393 17 Wu, C.-L. *et al.* Dietary fatty acid content regulates wound repair and the pathogenesis of
394 osteoarthritis following joint injury. *Annals of the rheumatic diseases* **74**, 2076-2083
395 (2015).

396 18 Schmitz, N., Laverty, S., Kraus, V. & Aigner, T. Basic methods in histopathology of joint
397 tissues. *Osteoarthritis and cartilage* **18**, S113-S116 (2010).
398 19 Wang, M. *et al.* MMP13 is a critical target gene during the progression of osteoarthritis.
399 *Arthritis research & therapy* **15**, 1-11 (2013).
400 20 Shen, J. *et al.* Deletion of the transforming growth factor β receptor type II gene in
401 articular chondrocytes leads to a progressive osteoarthritis‐like phenotype in mice.
402 *Arthritis & Rheumatism* **65**, 3107-3119 (2013).
403 21 Roach, H. I. *et al.* Association between the abnormal expression of matrix‐degrading
404 enzymes by human osteoarthritic chondrocytes and demethylation of specific CpG sites
405 in the promoter regions. *Arthritis & Rheumatism: Official Journal of the American*
406 *College of Rheumatology* **52**, 3110-3124 (2005).
407 22 Kawarai, Y. *et al.* Changes in proinflammatory cytokines, neuropeptides, and microglia
408 in an animal model of monosodium iodoacetate‐induced hip osteoarthritis. *Journal of*
409 *Orthopaedic Research®* **36**, 2978-2986 (2018).
410 23 Ford, C. A., Nowlan, N. C., Thomopoulos, S. & Killian, M. L. Effects of imbalanced
411 muscle loading on hip joint development and maturation. *Journal of Orthopaedic*
412 *Research* **35**, 1128-1136 (2017).
413 24 Draovitch, P., Edelstein, J. & Kelly, B. T. The layer concept: utilization in determining
414 the pain generators, pathology and how structure determines treatment. *Current reviews*
415 *in musculoskeletal medicine* **5**, 1-8 (2012).
416 25 Bunker, T., Esler, C. & Leach, W. Rotator-cuff tear of the hip. *The Journal of Bone and*
417 *Joint Surgery. British volume* **79**, 618-620 (1997).

418 26 Kagan 2nd, A. Rotator cuff tears of the hip. *Clinical orthopaedics and related research*,
419 135-140 (1999).
420 27 Kingzett-Taylor, A. *et al.* Tendinosis and tears of gluteus medius and minimus muscles as
421 a cause of hip pain: MR imaging findings. *AJR. American journal of roentgenology* **173**,
422 1123-1126 (1999).
423 28 Nepple, J. J., Thomason, K. M., An, T. W., Harris-Hayes, M. & Clohisy, J. C. What is the
424 utility of biomarkers for assessing the pathophysiology of hip osteoarthritis? A systematic
425 review. *Clinical Orthopaedics and Related Research*® **473**, 1683-1701 (2015).
426